Computer simulation of electrostatic aperture lens systems for electron spectroscopy

Article *in* Journal of Electron Spectroscopy and Related Phenomena · December 2009

DOI: 10.1016/j.elspec.2009.08.004

CITATIONS
14

READS
1,160

4 authors, including:

Melike Ulu
Afyon Kocatepe University
33 PUBLICATIONS **344** CITATIONS
SEE PROFILE

Mevlut Dogan
Max Planck Institute for Nuclear Physics
88 PUBLICATIONS **668** CITATIONS
SEE PROFILE

Journal of Electron Spectroscopy and Related Phenomena 175 (2009) 76–86

Contents lists available at ScienceDirect

Journal of Electron Spectroscopy and Related Phenomena

journal homepage: www.elsevier.com/locate/elspec

Computer simulation of electrostatic aperture lens systems for electron spectroscopy

Omer Sise*, Nimet Okumus, Melike Ulu, Mevlut Dogan

Department of Physics, Science and Arts Faculty, Afyon Kocatepe University, 03200 Afyonkarahisar, Turkey

ARTICLE INFO

Article history:
Received 18 June 2009
Received in revised form 7 August 2009
Accepted 7 August 2009
Available online 15 August 2009

PACS:
41.75.–i
41.85.–p
41.85Ne

Keywords:
Electron optics
Electrostatic lenses
Aperture lenses
Cylinder lenses
Focal points
SIMION

ABSTRACT

The electron optical properties of electrostatic aperture lens systems are studied by means of computer simulations. The influence of the geometric parameters on the focal points, magnification, and aberration coefficients has been discussed. Special cases such as a zoom lens (i.e., a lens which would produce a beam of variable energy and magnification with fixed image distance) are considered. The results have been compared with multi-cylinder lenses. Although the cylinder lenses tend to be slightly superior to the aperture lenses, they are capable of operating over much wider ranges of final-to-initial energy, and due to their greater compactness and simplicity, they can represent a very high quality lens in terms of lens parameters.

1. Introduction

Computer simulation has become an important tool to understand the optics of charged particles, to analyze their performance and imaging properties and to improve design for future optical systems [1]. In practice, the use of electrostatic lenses is more common compared to magnetic and quadrupole lenses, these being more easily controlled and shielded. So far, various types of electrostatic lenses, generally based on cylindrically symmetric elements at different potentials, have been widely used in scientific instruments [2], including electron guns [3–5], energy analyzers [6–9], time-of-flight spectrometers [10,11], electron microscopes [12], and focused ion beam systems [13,14], to mention only a few examples.

In our previous study [15], we presented a computer analysis of the "multi-cylinder" electrostatic lenses. Another common geometry often encountered in electron optical devices is the aperture lenses [16–21]. Although lenses with more than three apertures are expected to be better for some purposes and to have properties that are more flexible than those of the simpler two- and three-aperture lenses, they have been studied less often. To our knowledge, no detailed comparison has been published on these lenses.

In the present work, electron optical properties of "multi-aperture" lens systems are investigated and compared with cylinder lenses. A long series of simulations has been performed for three-, four- and five- element designs to obtain practical guidelines and principles for the design and operation of such electrostatic lenses. The simulations were performed with the charged particle optics simulation program SIMION 3D 8.0 [22]. Clearly anyone who wants to design an electrostatic lens can obtain the program and find the focal properties of his or her design. The possible benefit of the present paper is that the designer will have some idea of what to expect: the graphs in the paper may give a starting point for the design.

2. Calculation methods

To calculate the optical properties of electrostatic lenses for electrons or charged particles in general one must determine the potential distributions and fields throughout the region of interest, and trace particles through these fields. By calculating the trajectories of many particles one can see the beam trajectories in the lens directly. The optical properties are then determined by the way in which the electric field affects the trajectories of the parti-

* Corresponding author.
E-mail address: omersise@aku.edu.tr (O. Sise).

0368-2048/$ – see front matter © 2009 Elsevier B.V. All rights reserved.
doi:10.1016/j.elspec.2009.08.004

cles. Therefore, the focal points, lens magnification, and aberration coefficients can be determined from direct ray-tracing results.

In this work, the numerical simulations of the aperture lens systems have been performed using the program SIMION. This program is a powerful tool for numerical calculations of the electrostatic fields for a system of electrodes. The program uses the finite-difference method to numerically solve the Laplace equation, called over-relaxation. Simulation has been carried out on a two-dimensional grid (10 points per mm resolution [24]). SIMION is also able to calculate the charged particle trajectories in the system of electrostatic fields. Once the potential is obtained at each point, the trajectories are calculated through the lens by integrating the system of Newton's equations. A highly modified fourth-order Runge–Kutta technique is used for numerical integration of the trajectory in three dimensions.

SIMION 8.0 supports user-written programs that allow programmatic access to and control over most properties of electrons and fields, as well as timing and computational parameters. In this way, randomization of initial electron properties, optimization of lens voltages, and computing lens characteristics such as focal points, magnification, and spherical and chromatic aberration coefficients are possible. Many of the calculated results given in the following sections make use of user-written programs.

2.1. Lens geometry and potential

There are unlimited ways to configure aperture lenses. Perhaps the simplest studied geometry consists of two circular apertures of equal diameter [17]. Two-aperture lenses necessarily change the beam energy and produces a focus only at one ratio of final-to-initial energies. These limitations are avoided by using three or more lens elements [18,19,25]. Additional lens elements also facilitate a reduction in lens aberrations [21,26].

A three-aperture lens configuration is shown in Fig. 1(a). This lens system consists of three coaxial apertures of the same diameter D, separated by a distance A (note that for cylinder lenses 'A' is the length of the center electrodes including half the gap to each side). Since the behavior of the lens scales uniformly, all distances are quoted relative to the inside diameter of the apertures, D. This allows the results obtained here to be applied to a variety of designs. The relative value of A/D is a variable parameter determining the multi-element lens configuration in the calculations. The thickness of the electrode T has less effect on the lens properties, and is fixed to be $0.05\,D$.

The apertures, which are made of conductive material, are held at potentials V_i with respect to a reference potential that corresponds to the zero of particle kinetic energy; i.e., the reference is chosen such that a particle of charge q will have kinetic energy qV when it is in a region of potential V.

A series of calculations have been performed with three-, four-, and five-aperture lenses in both the so-called einzel (or unipotential) mode, i.e., $V_{initial} = V_{final}$ and the voltage-asymmetric mode, i.e., $V_{initial} \neq V_{final}$. Fig. 1(a) shows the potential distribution of a three-aperture einzel lens. The potential is symmetric about the plane of symmetry located at the center of the lens. Einzel lenses have traditionally been used for high energy studies [13,14].

2.2. Electron optical properties

Electrostatic lenses are often designed with the aid of trajectory calculations in the paraxial approximation in which the angle and distance between the system's optical axis and the ray of interest are small. The representation of the cardinal points and the focal and mid-focal lengths of the einzel lens is shown in Fig. 1(b). This figure illustrates the nomenclature for ray-tracing in object and image space. Here, R is the reference plane that is usually chosen to be the mechanical symmetry plane of the lens, H_1 and H_2 are the first and second principal planes which serve as a convenient construct for drawing object and image rays, F_1 and F_2 are the first and second principal foci, and P and Q are conjugate object and image distances. The focal lengths, f_1 and f_2, are the distances from the principal focal points to the principal planes. The positions of these focal points are dependent on the voltage ratios of the elements that constitute the lens. The electron's trajectory, depicted as a ray, is shown crossing the optical axis at the image point a distance Q from the center of the lens. It can be seen that the linear magnification M is given simply by the ratio of final to initial beam diameter in the radial axis, r_2/r_1 (note that the linear magnification $M < 0$ for real images). The so-called angular magnification is similarly given by $M_\alpha = \alpha_2/\alpha_1$. Useful relationships can be derived from the lens geometry, i.e., similar triangles, to find the typical lens equations [27]. The product of the angular and linear magnification is always equal to $MM_\alpha = -f_1/f_2 = (V_{initial}/V_{final})^{1/2}$ (Helmholtz–Lagrange Law).

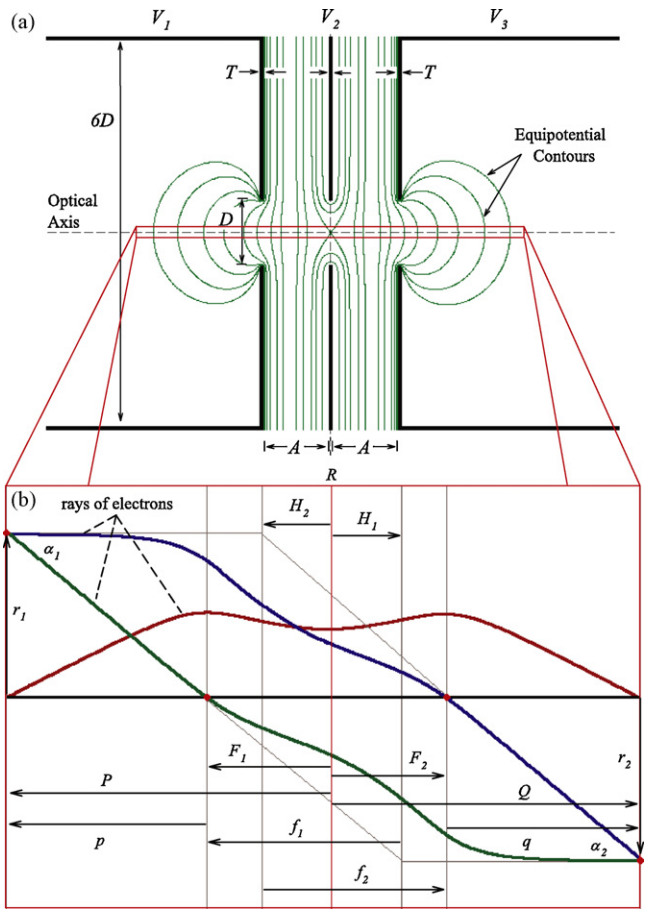

Fig. 1. (a) Cross-sectional diagram of a three-aperture electrostatic lens with equipotential contours ($T = 0.05D$; $A = 1.0D$). Here $V_1 = V_3$ and $V_2 = 10V_1$ is chosen, so the lens is an einzel lens. The potentials V_1 to V_3 are measured with respect to that of the cathode from which electrons originate. Equipotential lines (green) are drawn at different intervals of applied lens voltage. (b) The representation of the four cardinal points (red), and the focal and mid-focal lengths of the einzel lens is also shown. (For interpretation of the references to color in this figure legend, the reader is referred to the web version of the article.)

As in light optics, the optics of charged particles suffers from a number of image aberrations and distortions. Of primary concern are spherical and chromatic aberrations. In an electrostatic lens, spherical aberration is caused by the improper shape of the potential field of the lens which prevents the lens from functioning as a perfect lens. Analogously, chromatic aberration refers to the situa-

tion when otherwise identical particles of differing kinetic energies are not focused to the same point. Thus, an electrostatic lens with these aberrations cannot focus a point object to a point at the image plane. In order to determine the spherical and chromatic aberration coefficients, C_s and C_c, trajectories starting at different angle of incidence and different energies must be calculated through lens. The spherical aberration coefficients are obtained from $\Delta r = -MC_s\alpha_0^3$ [27], in which Δr is the radius of the disc formed in the Gaussian image plane by non-paraxial rays starting from an axial object point with a maximum half angle α_0, M is the linear magnification, and C_s is the third-order spherical aberration coefficient. Plotting Δr versus α_0^3 yields a straight line, allowing values for C_s to be found. Accuracy improves with increasing angle or distance away from center until higher-order aberrations begin to become manifest. Further, it can be shown that C_s is a fourth-order polynomial in $1/M$: $C_s(M) = C_{s0} + C_{s1}/M + C_{s2}/M^2 + C_{s3}/M^3 + C_{s4}/M^4$ [27].

The chromatic aberration coefficient in the image plane is described by $\delta r = -MC_c\alpha_0\delta V/V_0$ [27], where δr is the spread in image distance due to a spread in energies by $e\delta V$, and C_c is the chromatic aberration coefficient. We assumed that one ray with energy eV_0 crosses the axis at the image point, the higher energy ray with $e(V_0 + \delta V)$ crosses the axis at a distance δr above the axis. The same reasoning can be applied to find the chromatic aberration coefficient.

The aberrations of a lens can be reduced considerably by correct choice of number and structure of the electrodes. This was discussed by Harting and Read [16] and Renau and Heddle [23] who derived various figures of merit which may be used to compare the aberrations of different geometries. For the finite or infinite magnification case, the figure of merit g for a lens is given by $g = C_{s0}/f_2$. For the zero magnification condition, the figure of merit is slightly modified as $g_0 = C_{s4}F_2^2/f_1^3$. It is expected that a lens of three or more elements will have an appreciably smaller value of g and g_0 than any two element lens.

3. Results and discussion

We have carried out trajectory calculations of the electrons through three-, four-, and five-aperture lenses. The lens parameters such as focal lengths and magnification were computed for a series of aperture lens configurations. (The spherical and chromatic aberration coefficients were also computed but not given here in detail. They are available upon request. A full graphical analysis of aberrations would make the paper too complicated.) We have chosen two different ratios of the aperture spacing to the common aperture diameter, $A/D = 0.5$ and 1.0, to correspond to those given in Harting and Read [16]. In the following sections we are going to present the results of the numerical simulation.

3.1. Focal properties

3.1.1. Three-aperture lenses

The calculated values of the focal lengths for three-aperture lenses are shown in Figs. 2 and 3, for a wide range of values of

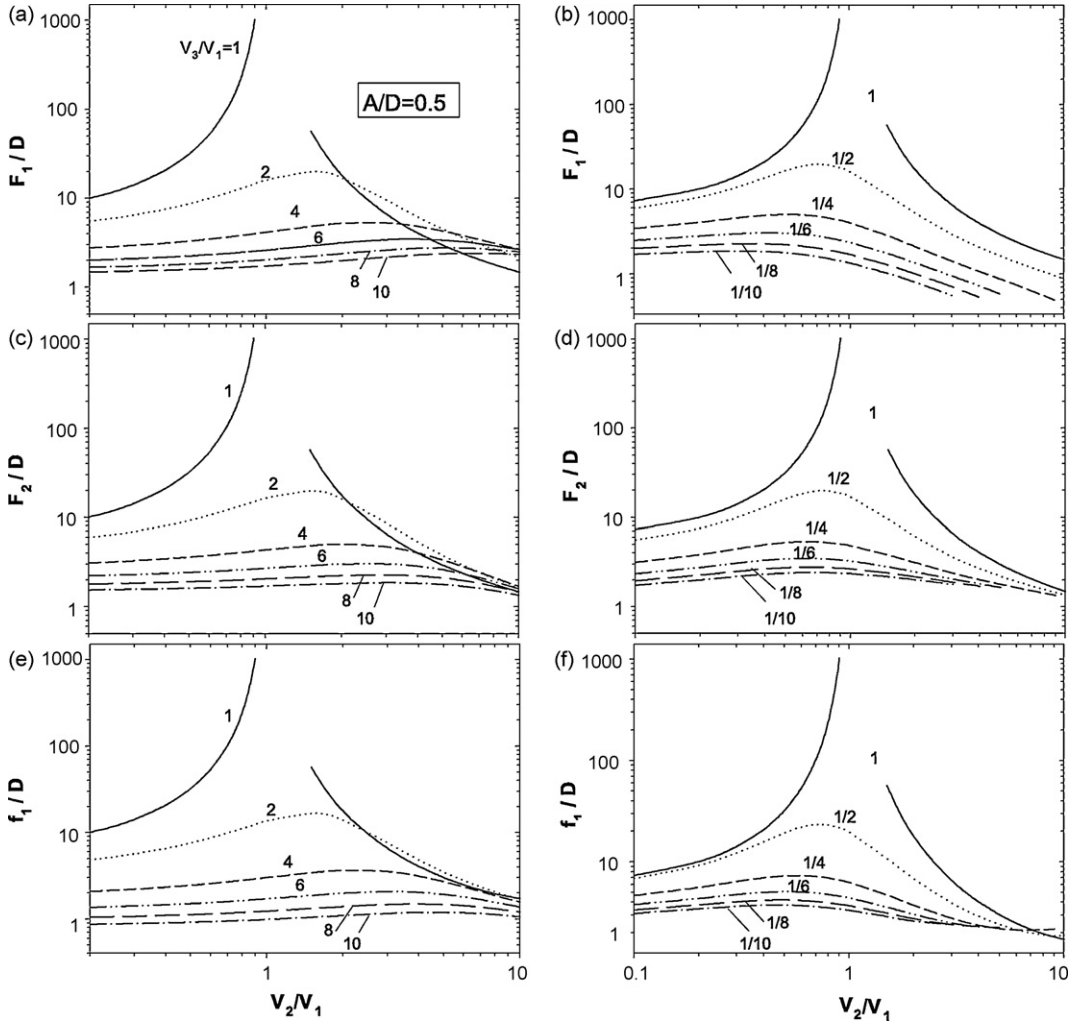

Fig. 2. Calculated values of the lens parameters for accelerating ($V_3/V_1 > 1$), decelerating ($V_3/V_1 < 1$), and einzel ($V_3/V_1 = 1$) lens having $A/D = 0.5$ as a function of V_2/V_1.

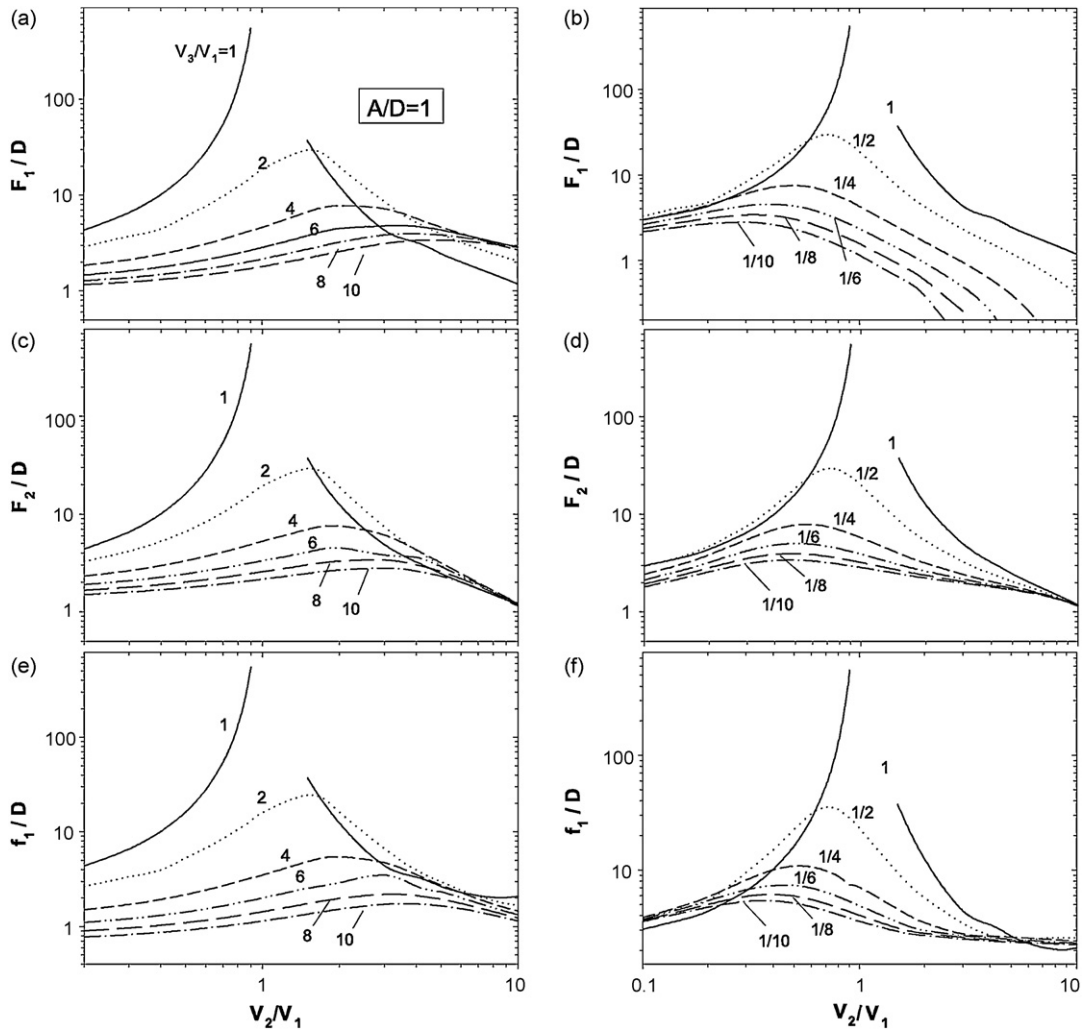

Fig. 3. Same as Fig. 2, but for $A/D = 1.0$.

the potentials (V_3/V_1 and V_2/V_1), and for $A/D = 0.5$ and 1. The second focal length, f_2, can be found using $f_2/f_1 = (V_3/V_1)^{1/2}$. It can be seen that as V_2/V_1 is increased from 0.1 to 10, the focal and mid-focal lengths pass through a maximum value and then decrease to a minimum value. This behavior is repeated when V_3/V_1 is varied from unity (< 1 or > 1), but f and F tend to become shorter and less dependent on V_2/V_1. These results are almost identical to those of cylinder lenses. The overall effect on the focal properties is not large.

In Table 1, both focal points and figures of merits are listed for different voltage ratios of V_2/V_1 for fixed $V_3/V_1 = 5$ and $A/D = 0.5$, and thus can be readily compared for both three-cylinder and three-aperture lenses. For both lenses g has the same value at $V_2 = V_1$ and $V_2 = V_3$ because in these cases the system reduces to a two-element lens. For $V_2 < V_1$ or $V_2 > V_3$, g becomes smaller, and the cylinder lens is the better one. For example, in the case of the three-cylinder lens the figure of merit g is listed as 7.01 for $V_2/V_1 = 5$ and 2.66 eV for $V_2/V_1 = 10$. Similarly, for the three-aperture lens these numbers are 7.89 and 3.83, respectively. If the lens differ in A/D value, the behavior is quite similar that cylinder lenses offer advantages over aperture lenses of the same inner diameter. For a given voltage ratio they are a little stronger and have smaller aberration coefficients. For $V_1 < V_2 < V_3$, $A/D = 0.5$ has smaller g, but for other ratios of V_2/V_1 the lens with $A/D = 1$ should be preferred. The same conclusion is also valid for g_0.

3.1.2. Four-aperture lenses

Figs. 4 and 5 show the calculated values of the lens parameters F_1 and F_2 for four-aperture lenses having the ratio A/D equal to 0.5 and 1.0, for ratios of V_2/V_1 from 0.1 to 10, for five dif-

Table 1
Values of the figure of merit for three-element lenses for $V_3/V_1 = 5$ and $A/D = 0.5$.

V_2/V_1	Cylinder $A/D = 0.5$						Aperture $A/D = 0.5$					
	f_1	F_2	C_{s0}	C_{s4}	g	g_0	f_1	F_2	C_{s0}	C_{s4}	g	g_0
0	1.04	1.68	12.2	3.16	5.24	7.92	1.50	2.37	22.1	5.14	6.59	8.53
0.5	1.40	2.22	20.9	4.51	6.65	8.07	1.85	2.87	30.3	6.22	7.31	8.06
1	1.76	2.71	27.5	5.16	7.01	7.01	2.17	3.29	35.3	6.66	7.29	7.10
2	2.20	3.22	30.4	5.81	6.17	5.63	2.56	3.73	38.4	7.38	6.71	6.11
5	1.76	2.21	27.5	5.16	7.01	4.67	2.26	2.95	39.9	7.44	7.89	5.58
10	1.05	1.07	6.24	0.98	2.66	0.98	1.47	1.65	12.9	1.93	3.93	1.64

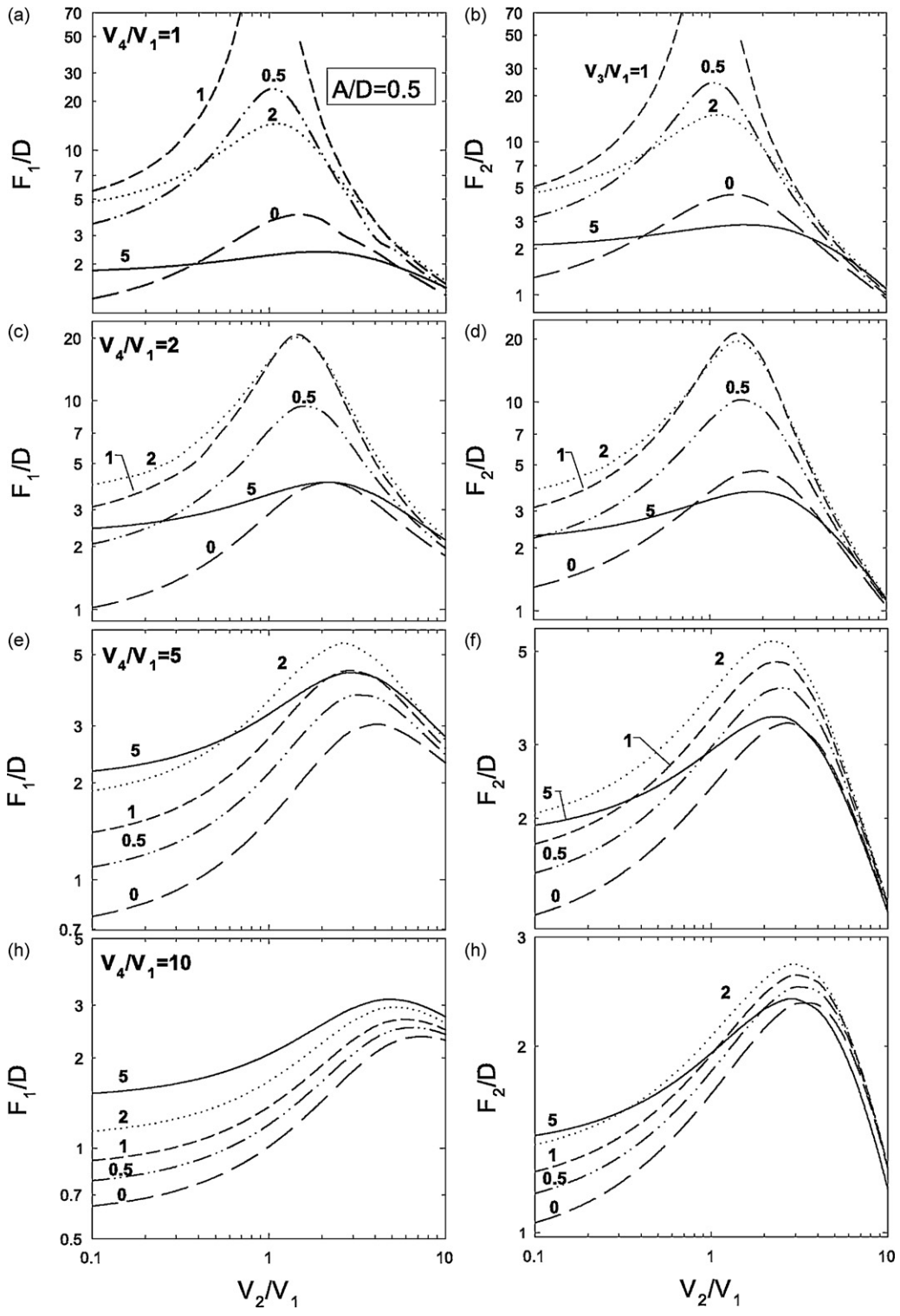

Fig. 4. Values of the first and second mid-focal lengths F_1/D and F_2/D for four-aperture lenses with $A/D = 0.5$ as a function of V_2/V_1 for different values of V_3/V_1 (on the curves) and V_4/V_1.

ferent values of V_3/V_1 from 0 to 5, and for four different values of V_4/V_1 from 1 to 10. Compared to cylinder lenses, the trend is very similar. Some values of g and g_0 for four-element lenses, extracted from the focal lengths and aberration coefficients, are shown in Table 2 for $V_4/V_1 = 1$, $V_3/V_1 = 5$ and $A/D = 0.5$. The overall effect on the focal properties is not large, but the lower aberration of the cylinder lens is quite noticeable. An increase in the accelerating potential ratio V_4/V_1 greatly reduces the lens aberrations. So it is clearly advantageous to use a four-element lens as a focusing lens. For $V_4/V_1 = 5$ four-element lenses give a smaller value of g and g_0 than the three-element lenses given in Table 1.

3.2. Zoom-lens properties

3.2.1. Three-aperture zoom lenses

In an electrostatic lens, it is very often desirable to be able to keep the image of a given object fixed when the final-to-initial energy

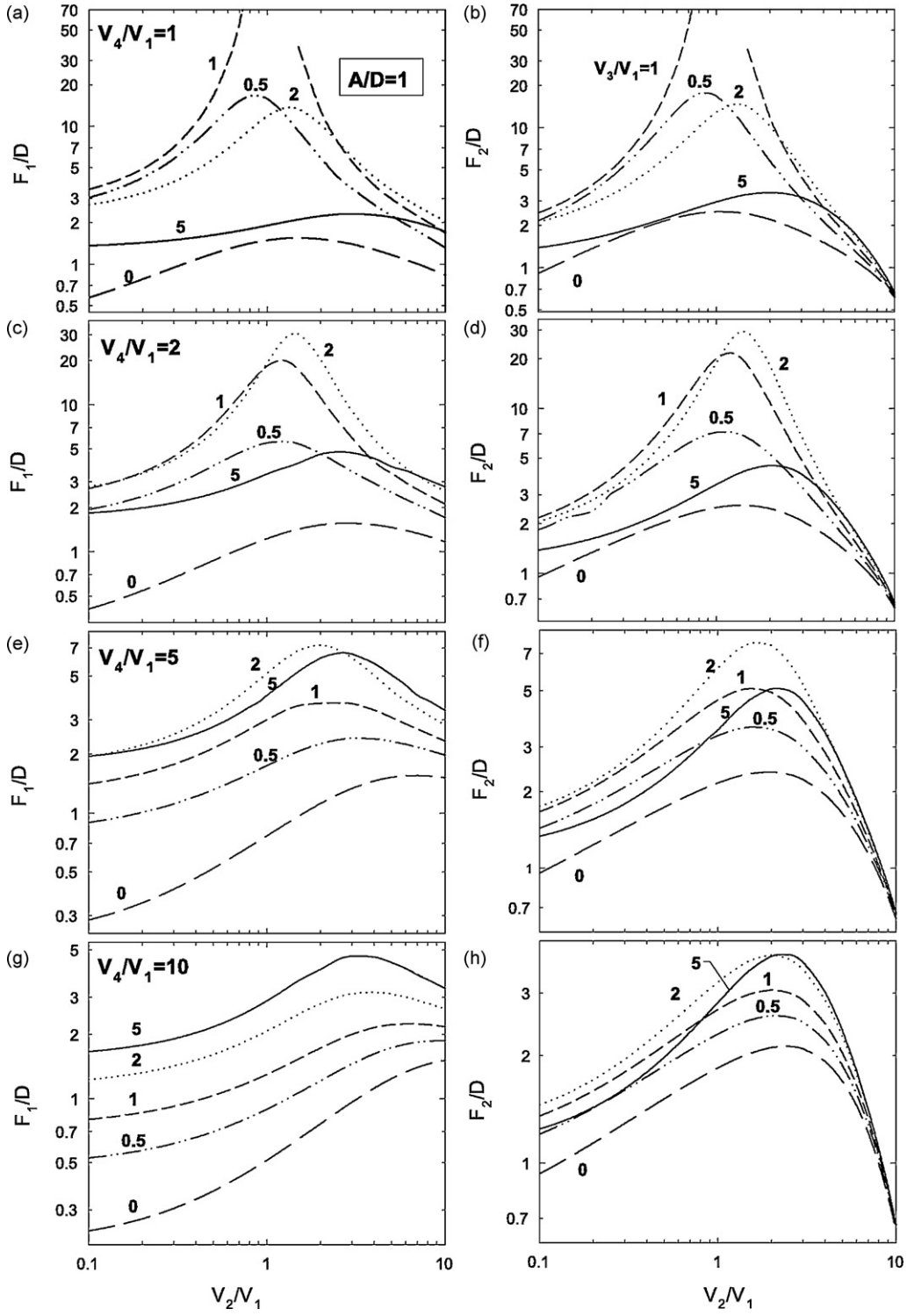

Fig. 5. Same as Fig. 4, but for $A/D = 1.0$.

is changed. A lens operated in this way is usually referred to as a *zoom* lens. Three-aperture lenses are often used with a fixed object distance P and a fixed image distance Q, and to maintain these fixed values, V_2/V_1 has to be varied as V_3/V_1 is varied. Fig. 6 shows these relationships for a pair of values of $P/D = 5$ and $Q/D = 5$, and for a value of $A/D = 1.0$.

A user program was used to measure the focus point size as a function of the two voltage ratios V_2/V_1 and V_3/V_1. The minima on the surface plot in Fig. 6 demonstrate where the lens is properly focused. Here, Δr is the beam diameter at the image plane. One can roughly see from the plots where the surface minima are, but it does not precisely identify the locations of the minima. Therefore, an optimization is necessary for this kind of calculation. The simplex optimization method is adopted in a user program to search optimal voltages for a given optical condition. This method is based on a conjugational gradient algorithm, so it converges very fast, and simplifies the optimizing procedure. The program uses a (Monte-Carlo) technique and optimization routine to precisely identify locations

Table 2
Values of the figure of merit for four-element lenses having $V_4/V_1 = 1$, $V_3/V_1 = 5$, and $A/D = 0.5$.

V_2/V_1	Cylinder $A/D = 0.5$						Aperture $A/D = 0.5$					
	f_1	F_2	C_{s0}	C_{s4}	g	g_0	f_1	F_2	C_{s0}	C_{s4}	g	g_0
0	1.54	1.56	9.33	16.9	6.06	11.3	1.94	2.02	16.4	25.8	8.45	14.4
0.5	1.87	1.99	14.3	18.5	7.66	11.3	2.32	2.49	23.3	28.3	10.0	14.0
1	2.09	2.25	17.7	17.7	8.49	9.91	2.57	2.77	27.4	27.0	10.7	12.2
2	2.22	2.34	18.0	14.0	8.12	7.03	2.70	2.85	25.7	21.0	9.52	8.65
5	1.83	1.58	7.01	7.01	3.84	2.89	2.19	1.97	9.34	9.34	4.26	3.43
10	1.44	0.78	2.53	3.58	1.76	0.73	1.77	1.09	3.10	4.05	1.75	0.87

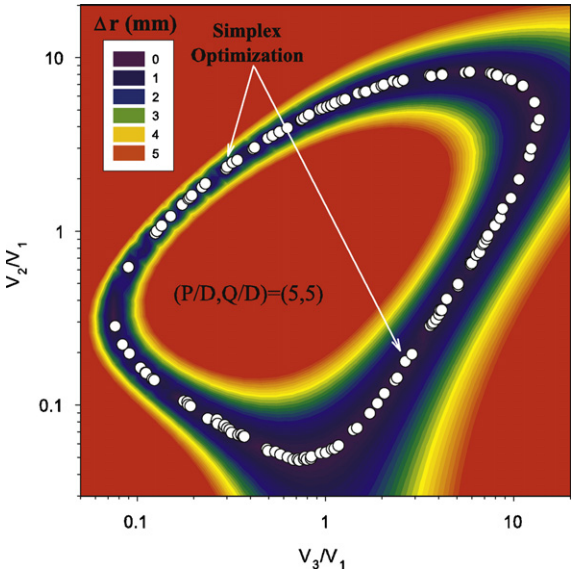

Fig. 6. A 2D surface plot of beam diameter as a function of V_2/V_1 and V_3/V_1 for a three-aperture lens having $P/D = 5$, $Q/D = 5$, and $A/D = 1.0$. A simplex optimization was used to precisely identify locations of some representative set of minima (circles).

of some representative set of minima. These minima are shown as a circle.

The procedure described above was repeated for different values of the object distance P and image distance Q for three-aperture lenses. In Fig. 7(a)–(c), we calculated zoom-lens curves for three different values of $A/D = 0.5$, 1.0 and 2.0, and for fixed values of the object and the image distance $P/D = 3.5$ and $Q/D = 2.5$. Fig. 7(d)–(f) shows the relationship between V_2/V_1 and V_3/V_1 for three different values of the image distance $Q/D = 2.8$, 4 and 10, for a fixed value of $P/D = 3.5$ and $A/D = 1.0$. A representative variation of the linear magnification is also shown in these figures.

The shapes of the zoom-lens curves are remarkably similar with cylinder lenses. But, there are some differences. Aperture lenses are 'weaker' requiring a higher V_2/V_1 ratio for a given object and image distance for a fixed V_3/V_1. Since the aberrations are usually lower for the higher values of V_2/V_1, these lenses are expected to have lower aberration coefficients than cylinder lenses. Table 3, compiled from data presented in Fig. 7(a), illustrates this behavior for the three-element cylinder and aperture lens both having $A/D = 0.5$ for $P/D = 3.5$ and $Q/D = 2.5$. Here, C_s and C_c are the spherical and chromatic aberration coefficient defined for finite magnification. As previously shown in Table 1, cylinder lenses have better aberration properties for the same voltage ratios of V_2/V_1 and V_3/V_1. In addition, the lens with $A/D = 1$ tends to have lower aberration coefficients and offers a wide range of magnifications than the lens having $A/D = 0.5$.

3.2.2. Four-aperture zoom lenses

If it is required to maintain both the image position and magnification constant while the energy of the image is varied, the lens must have at least four elements [21]. The four-aperture lens has three degrees of freedom (three potential ratios). One degree of freedom is used to set the ratio of final-to-initial energy, the second to fix the focal points. The third degree of freedom may be used to control the magnification (linear or angular).

A user program was used to automatically vary the second and third voltages of the four-aperture lens to maintain constant object and image positions and linear magnification (P, Q and M). Table 4 shows the fixed values of P, Q and M for the six sets that we have studied. The calculated values of V_2/V_1 and V_3/V_1 for $A/D = 0.5$ and 1 are shown in Fig. 8 as a function of V_4/V_1. The highest values of V_3/V_1 gives the smallest aberration coefficients, and so we have searched for this type of working point for all the combinations. When it exists over only a small range of values of V_4/V_1, we give, instead, data that have the lowest values of V_3/V_1.

The ranges of values of V_4/V_1 are considerably wider than those available with the four-cylinder lens. The smallest range for the four-aperture lens, from $V_4/V_1 = 1$ to 10, occurs when $(P, Q, M) = (3, 3, 1)$ for $A/D = 0.5$, and $(P, Q, M) = (4, 4, 1)$ for $A/D = 1.0$. As shown in Table 5, increasing V_4/V_1 has the effect of reducing the aberration coefficients of the lens, and the minimums of coefficients are significantly smaller than those of the three-element lens. In general, lens with $A/D = 1$ appears to provide a good overall design, giving focussing power at a low voltage. Calculated values of the mid-focal length, F_1, as a function of V_4/V_1 are also given in Fig. 9 for each of the six sets. If F_1 is known for a constant (P,Q,M) set then the remaining lens parameters (f_1, f_2, F_2) can be obtained from the lens equation [27].

Table 3
Zoom-lens properties of the three-element cylinder and aperture lens having $A/D = 0.5$ for $P/D = 3.5$ and $Q/D = 2.5$

V_3/V_1	Cylinder $A/D = 0.5$				Aperture $A/D = 0.5$			
	V_2/V_1	M	C_s	C_c	V_2/V_1	M	C_s	C_c
1/5	−0.01	1.18	729	42.6	−0.09	1.16	685	47.2
	2.39	0.79	531	33.8	3.78	0.76	269	21.5
1	−0.22	0.72	1353	31.0	−0.34	0.72	1135	33.3
	6.97	0.73	137	6.02	9.63	0.72	75	4.54
5	−0.11	0.44	495	10.6	-0.47	0.44	455	11.5
	10.45	0.65	77	4.09	15.5	0.68	39	2.81

Table 4
Fixed lens parameters for four-cylinder and four-aperture lenses having a constant object and image distance and magnification, together with the ranges of values of V_4/V_1.

		No					
		1	2	3	4	5	6
$A/D = 0.5$	P/D	2	2	2	2	3	4
	Q/D	2	3	4	4	3	2
	M	1	1	1	2	1	0.5
Cylinder [a]	V_4/V_1	1–29	2–30	6–32	1–14.5	1–7	1–6.8
Aperture [b]	V_4/V_1	1–45	15–60	15–60	1–25	1–10	1–11
$A/D = 1.0$	P/D	3	3	3	3	4	5
	Q/D	3	4	5	5	4	3
	M	1	1	1	2	1	0.5
Cylinder [a]	V_4/V_1	1–23	1–30	7–30	1–9	1–10	1–15
Aperture [b]	V_4/V_1	1–55	1–62	10–62	1–18	1–17	1–23

[a] Ref. [15].
[b] Present work.

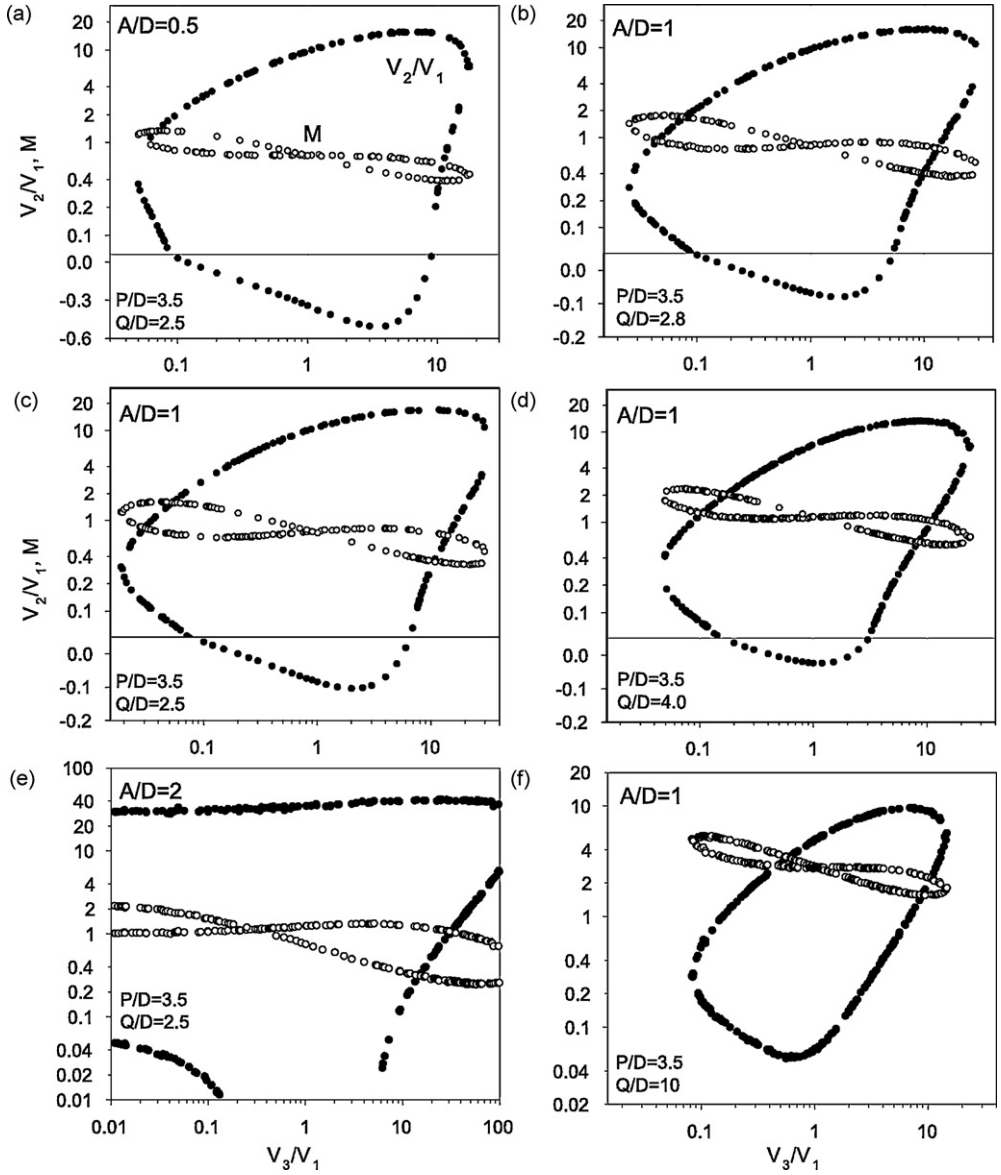

Fig. 7. Relationship between V_2/V_1 and V_3/V_1 (●) and variation of the magnification M (○) with V_3/V_1 (zoom-lens curves) (a)–(c) in three-aperture lenses having a constant object and image distance, $P/D = 3.5$ and $Q/D = 2.5$ for $A/D = 0.5$, 1 and 2, and (d)–(f) for various fixed image distance for $A/D = 1$ for $Q/D = 2.8$, 4 and 10, respectively. Note that the vertical scales are linear for negative values.

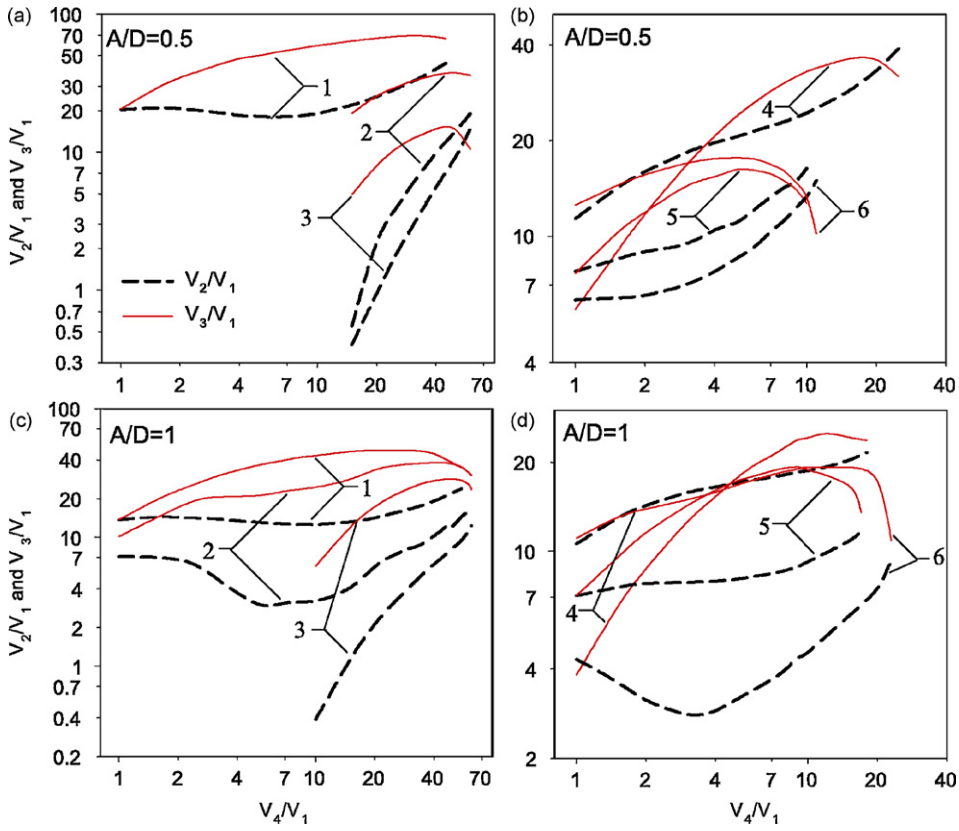

Fig. 8. Relationship between voltage ratios V_2/V_1 and V_3/V_1 for $A/D = 0.5$ (a) and (b) and for $A/D = 1$ (c) and (d), as a function of V_4/V_1 for six combinations of P, Q and M specified in Table 4.

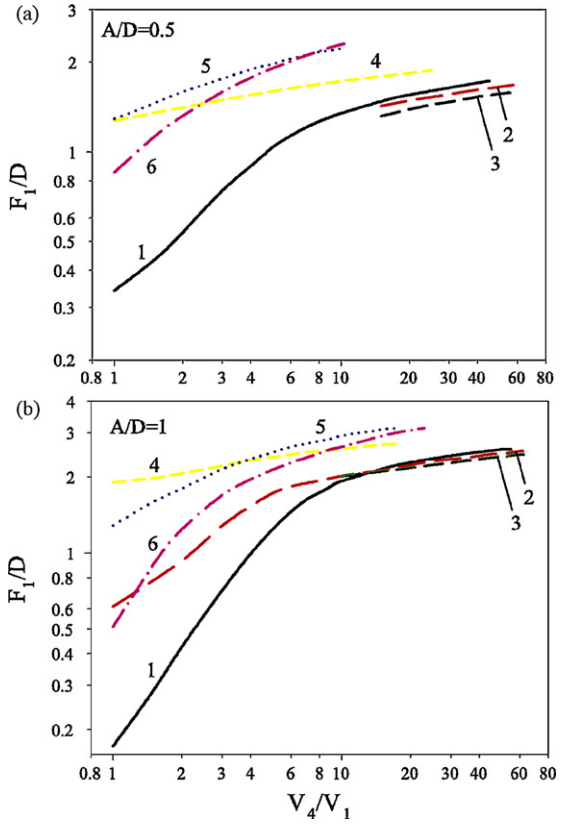

Fig. 9. Values of the first mid-focal length F_1/D for four-aperture lenses with $A/D = 0.5$ (a) and 1 (b) as a function of V_4/V_1 for six combinations of P, Q and M.

3.2.3. *Five-aperture zoom lenses*

Fig. 10 shows a schematic diagram of a five-aperture lens consisting of two three-aperture lenses with a common middle lens element. The lens in Fig. 10 has dimensions $A/D = 0.5$ and $L/D = 1$ ($P/D = Q/D = 3$). We have studied this lens and also the rather longer one with $A/D = 1.0$ and $L/D = 2$ ($P/D = Q/D = 4$).

The four free lens voltages in a five-element lens define a multi-dimensional parameter space, which may contain many different lens operating modes [28,29]. Therefore, the use of a five-aperture system allows extra degrees of freedom when focusing the electron beam to an image point. In addition five-aperture lenses can produce a parallel (afocal) beam of electrons. An afocal lens consists of two identical three-element lenses arranged so that the second focal point of the first lens (F_2) and the first focal point of the second lens (F_1) coincide. But, in this case, the length of the center electrode must be long enough ($L/D \geq 3$ for $A/D = 0.5$ and $L/D \geq 4$ for $A/D = 1.0$) so that the distance $F_2 - F_1$ is equal to the distance between the reference planes of the lenses.

To analyze the behavior of five-aperture lenses as the overall voltage ratio V_5/V_1 varies, we have used a simple minimization routine to find the values of V_2/V_1 and V_4/V_1. We show our results

Table 5
Zoom-lens properties of the four-element cylinder and aperture lens having $A/D = 0.5$ for $P/D = 3$, $Q/D = 3$, and $M = 1$.

V_4/V_1	Cylinder $A/D = 0.5$				Aperture $A/D = 0.5$			
	V_3/V_1	V_2/V_1	C_s	C_c	V_3/V_1	V_2/V_1	C_s	C_c
1	5.77	5.82	41.9	3.86	7.63	7.74	25.5	2.35
2	8.77	6.83	28.2	2.71	11.9	8.94	17.0	1.63
3	10.3	7.42	24.8	2.48	14.3	9.44	14.6	1.46
4	10.9	8.01	23.5	2.40	15.4	10.5	13.5	1.38
5	10.9	8.74	23.1	2.36	16.2	11.1	12.9	1.32

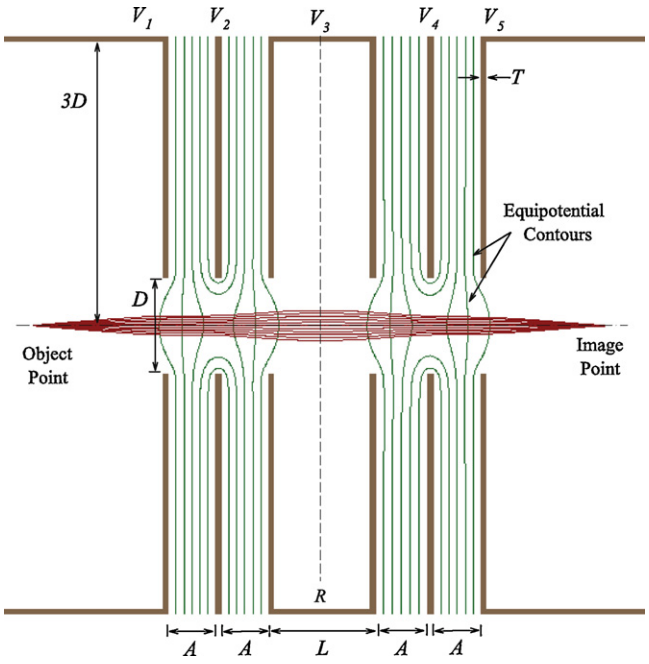

Fig. 10. Cross-sectional diagram of a five-aperture lens. The potentials V_1 to V_5 are measured with respect to that of the cathode.

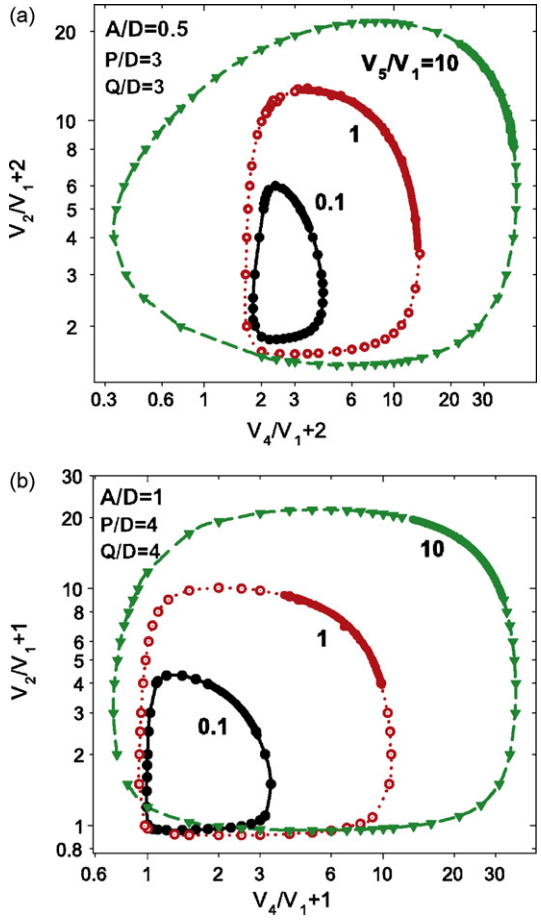

Fig. 11. Variation of the magnification M as a function V_2/V_4 which contains two voltage ratios of middle electrodes for five-aperture lenses having $A/D = 0.5$ (a) and 1 (b).

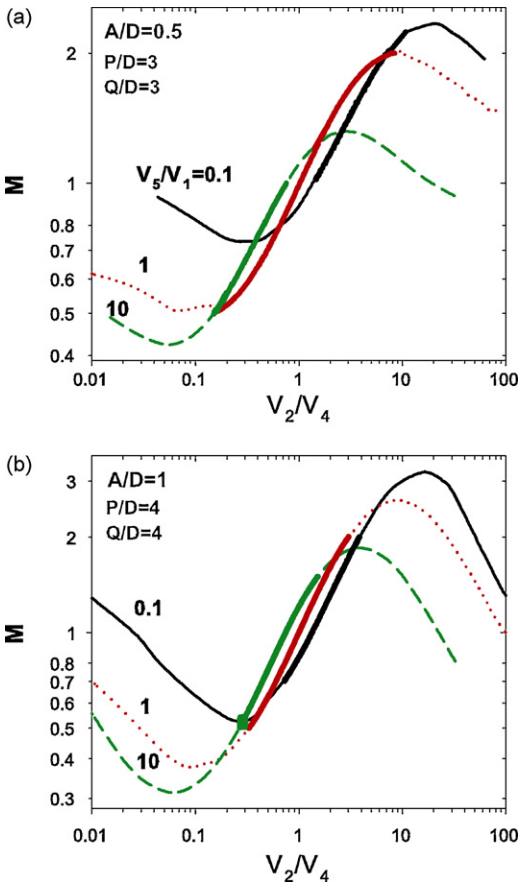

Fig. 12. Values of V_2/V_1 and V_4/V_1 for five-aperture lenses having $A/D = 0.5$ (a) and 1 (b).

for both lenses with $V_5/V_1 = 1/10$, 1 and 10 in Fig. 11. The dependence of the magnification M on the overall voltage ratio is shown in Fig. 12. Some regions are indicated by the thick solid curves in these figures. In all cases the potential of the center electrode, V_3, is set such that $V_3/V_1 = (V_5/V_1)^{1/2}$.

Similar curves apply for other values of V_5/V_1. Fig. 13 shows various zoom-lens curves as V_2/V_1 and V_4/V_1 are varied over a large range. In each curve, the optimized relationship between these two voltages were found for a given V_5/V_1. The range of the magnifica-

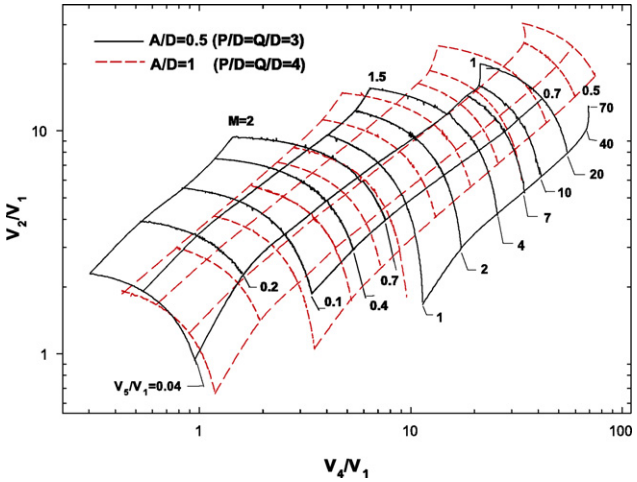

Fig. 13. Design curves of constant magnification and overall voltage ratio for two different type of five-aperture lens.

tion is from 0.5 to 2 and this range for V_5/V_1 is from 0.04 to 70 (a total span of $\sim 1 : 10^3$). The use of five-aperture lens is advantageous in that constant magnification (and hence transmission) can be ensured over a wide final-to-initial energy range while maintaining constant image and object positions. The results also show that it is possible to obtain small aberration coefficients for five-aperture lenses.

4. Summary and conclusion

In this paper, the focal properties of multi-aperture lenses were investigated over ranges of values of the lens parameters and compared with multi-cylinder lenses. Aperture lenses are expected to be used as a focussing lens for apparatuses using electron beams, particularly for electron scattering apparatus. The reason for this is that electrostatic aperture lenses can be made compact and light.

Cylinder lenses have the advantage that in comparison with aperture lenses the spherical and chromatic aberration are smaller for a given lens diameter. This is the consequence of the smoother axial potential distribution. The lens having $A/D = 1$ offers the advantage of a slightly wider range of magnifications and small aberrations compared with $A/D = 0.5$ for the same object and image distance.

However, it is not yet clear the extent to which type of lenses is more desirable over the other. This largely depends on the specific application and the overall length of the lens system employed. Nevertheless, computer optimization of electrostatic lenses is certainly important. This will save time and resources in design of future charged particle optical systems.

Using the ideas arising from this and our previous studies, the following conclusions can now be drawn regarding the design of electrostatic lens systems. The number of electrodes employed in the lens system, either for extraction or imaging, should ideally not be lower than 3. A lens with three electrodes will generally be able to operate only over a quite limited range in $V_{initial}/V_{\text{final}}$. To provide more flexibility, both in terms of energy range and for optimization with respect to optical properties, more independent lens elements have to be added. If more degrees of freedom are desirable, it is probably better to use some combination of such basic units separated by field-free regions than to design a lens where more electrodes are closely spaced.

In energy scanning procedure of the lens, the magnification and the image point should be fixed over the whole electron kinetic energy range. In this case one desires to continuously change only one potential in order to focus successive kinetic energy groups of electrons. In an experiment, if it is possible to maintain the successive voltage ratios constant, each lens can then be suitably polarized by means of voltage dividers. In this way, the problem becomes that of finding for one lens an object distance P such that the corresponding image distance Q remains constant while the final beam energy varies in a fixed domain.

Acknowledgements

The authors would like to thank Professor Genoveva Martinez Lopez for helpful discussions. We also thank David J. Manura for useful suggestions on user programming in SIMION 8.0.

References

[1] I.W. Drummond, Vacuum 34 (1984) 51–61.
[2] J.H. Moore, C.C. Davis, M.A. Caplan, Building Scientific Apparatus, Addison Wesley, London, 1983.
[3] M.T. Bernius, K.F. Man, A. Chutjian, Rev. Sci. Instrum. 59 (11) (1988) 2418–2423.
[4] L. Boesten, K. Okada, Meas. Sci. Technol. 11 (2000) 576–583.
[5] S. Raj, D.D. Sarma, Rev. Sci. Instrum. 75 (2004) 1020–1025.
[6] N. Mårtensson, P. Baltzer, P.A. Brhwiler, J.-O. Forsell, A. Nilsson, A. Stenborg, B. Wannberg, J. Electron Spectrosc. Relat. Phenom. 70 (1994) 117–128.
[7] S. Shiraki, H. Ishii, M. Owari, Y. Nihei, J. Electron Spectrosc. Relat. Phenom. 88–91 (1998) 1021–1026.
[8] F. Offi, A. Fondacaro, G. Paolicelli, A. De Luisa, G. Stefani, Nucl. Instrum. Method Phys. A 550 (2005) 454–466.
[9] E.P. Benis, T.J.M. Zouros, J. Electron Spectrosc. Relat. Phenom. 163 (2008) 28–39.
[10] R. Antoine, L. Arnaud, M. Abd El Rahim, D. Rayane, M. Broyer, Ph. Dugourd, Int. J. Mass Spectrom. 239 (2004) 1–6.
[11] D. Papanastasiou, A.W. McMahon, Int. J. Mass Spectrom. 254 (2006) 20–27.
[12] M. Mankos, D. Adler, L. Veneklasen, E. Munro, Phys. Procedia 1 (1) (2008) 485–504.
[13] S. Nomura, J. Vac. Sci. Technol. A 16 (1) (1998) 104–108.
[14] S. Nomura, J. Vac. Sci. Technol. A 17 (1) (1999) 82–85.
[15] O. Sise, M. Ulu, M. Dogan, Nucl. Instrum. Methods Phys. A 554 (2005) 114–131.
[16] E. Harting, F.H. Read, Electrostatic Lenses, Elsevier, Amsterdam, 1976.
[17] F.H. Read, J. Phys. E: Sci. Instrum. 2 (1969) 165–169.
[18] F.H. Read, J. Phys. E: Sci. Instrum. 2 (1969) 679–684.
[19] F.H. Read, J. Phys. E: Sci. Instrum. 3 (1970) 127–131.
[20] K. Shimizu, H. Kawakatsu, J. Phys. E: Sci. Instrum. 7 (1974) 472–476.
[21] G. Martinez, M. Sancho, Nucl. Instrum. Methods Phys. Res. A 298 (1990) 70–77.
[22] Simion 3D v8.0, Scientific Instrument Services Inc. www.simion.com.
[23] A. Renau, D.W.O. Heddle, J. Phys. E 19 (1986) 288–295.
[24] T.J.M. Zouros, O. Sise, F.M. Spiegelhalder, D.J. Manura, Int. J. Mass Spectrom. 261 (2007) 115–133.
[25] R.E. Imhof, F.H. Read, J. Phys. E: Sci. Instrum. 1 (1968) 859–860.
[26] O. Sise, M. Ulu, M. Dogan, Nucl. Instrum. Methods Phys. A 573 (2007) 329–339.
[27] D.W.O. Heddle, Electrostatic Lens Systems, 2nd edn., IOP Press, London, 2000.
[28] D.W.O. Heddle, J. Phys. E: Sci. Instrum. 4 (1971) 981–983.
[29] D.W.O. Heddle, N. Papadovassilakis, J. Phys. E: Sci. Instrum. 17 (1984) 599–605.